University of Exeter coursework header sheet

ECM3101 Individual Project (Beng) (A, TRM1+2 2015/6)

004707

1019472

630025821

Coursework: Final Report

Submission Deadline: Thu 28th Apr 2016 12:00

Personal tutor: Professor Gavin Tabor

Marker name: G Tab

Word count: 6510

By submitting coursework you declare that you understand and consent to the University policies regarding plagiarism and mitigation (these can be seen online at www.exeter.ac.uk/plagiarism, and www.exeter.ac.uk/mitigation respectively), and that you have read your school's rules for submission of written coursework, for example rules on maximum and minimum number of words. Indicative/first marks are provisional only.

Final Report

Investigating the Internal Temperature Distribution of a Hot Cornish Pasty Subjected to Forced Convection Through Theoretical, Experimental and Computational Analysis

Oliver Nield

2016
3rd Year Individual Project

I certify that all material in this thesis that is not my own work has been identified and that no material has been included for which a degree has previously been conferred on me.

Signed.....Oliver Nield.

College of Engineering, Mathematics, and Physical Sciences
University of Exeter

Final Report

ECM3101

Title: Investigating the Internal Temperature Distribution of a Heated Cornish Pasty Subjected to Forced Convection Through Theoretical, Experimental and Computational Analysis

Word count: 6510

Number of pages: 26

Date of submission: Thursday, 28 April 2016

Student Name: Oliver Nield

Programme: Mechanical Engineering

Student number: 630025821

Candidate number: 004707

Supervisor: Gavin Tabor

Abstract

The aim of this project is to create a CFD model of a pasty that is subjected to forced convection and can then be analysed to find the internal heat distribution. The purpose for this is to provide information on the effectiveness of the current cooling facilities at Ginsters where pasties are passed through a spiral cooler while being blown by-28°C at 10m/s. The aim was achieved through an iterative modelling process, commencing with simplified models that could be validated through theoretical and experimental analysis and then developed into more complex and accurate models.

The results of the final CFD showed that the temperature was not distributed in the complex model same manner as in the simplified models and an ineffectiveness of the air to cool the centre of the pasty. Upon investigation it was determined that there was an air pocket inside the pasty that acted as an insulator and vastly reduced the effectiveness of the cooling air. The key information includes a brief background description, project aims, methodologies used, main outcomes and how these agree with the aims, and conclusions. This result could not however be validate with experimental work due to limited facilities and so additional work will have to be carried out to verify this situation and quantify the effects of it.

Keywords: CFD, Heat Distribution, Food

Table of contents

1. Introduction and background

Ginsters is a UK food producer based in the south-west of England that specialises in making mass-produced Cornish pasties, among other products. It currently uses a helical cooling tower to cool the pasties that they produce. Once the pasties leave the oven they travel down a spiral pathway with three fans blowing -28°C air at 10m/s across the top of the pasties until they reach the bottom and are transported for packaging. This project will investigate the effects of airflow over a hot pasty in an attempt to observe the temperature distribution and to discover if the air cools the pasty evenly.

The aim of this project is to create a CFD model of a hot pasty being subjected to the same airflow conditions as found in the Ginsters cooling tower in order for it to be analysed. This will be achieved through an iterative modelling process with the pasty being firstly modelled as a simple hemisphere. The pasty will then be modelled with increasing complexity until it is modelled as composite pasty comprised of pastry, a meat filling and an air pocket. The purpose of commencing the investigation with a simplified model is to validate aspects of the CFD using theoretical and experimental techniques that could not be carried out on a complex model.

The reason the validation techniques could not be used on the complex model are twofold, firstly, there are no established theoretical methods for analysing the temperature distribution over the complex geometry of a pasty. Secondly, the extreme conditions in the cooling tower could not be recreated using university experimental facilities. Using a hemisphere as a simplified model and reducing the extreme temperatures of the pasty and airflow allows both of these problems to be overcome. The results of the simulation of the simplified model can be compared with the theoretical and experimental results and if they correspond well at the lower temperatures it can be assumed that the simulation will be accurate with the actual conditions. Simulations with the complex geometry can then be checked by comparing it to the simplified model.

The objective of this project is to successfully validate the CFD simulation of the composite pasty by comparing the temperature distribution and the airflow velocities to previous simulations that were, in turn, validated through theoretical and experimental results.

2. Literature review

The initial research for this project was into the process of heat transfer with the aim of determining the mechanism causing the heat loss in the pasties. The results from this research where then used to conduct research into suitable theoretical solutions to the problem being investigated. Finally current CFD techniques used in food processing were evaluated to determine techniques to improve the quality of the simulations in the project.

Yunus A Cengel [1] discusses heat transfer and the relationship between conduction and convection in a flowing fluid. He states that when dealing with heat transfer problems in fluids there is a combination of radiation and either conduction, if the fluid is stationery, or convection, if the fluid is in motion. The reason that both are not considered is that convection can be viewed as a combination of conduction and fluid motion, and conduction can be viewed as convection with no fluid motion, they are, therefore, simply the same physical mechanism operating under different conditions. In the case being studied the heat transfer through radiation can be neglected as it is insignificant compared to the convective heat transfer at low temperatures [2]. In the case being studied in this project the fluid is in motion and so the heat transfer will be through convection.

Singal [3] states that there are two types of convection, free and forced convection, free convection occurs when fluid motion is only caused by temperature differences in the fluid and forced convection occurs when there is an external force driving the fluid motion. In this investigation the air is being driven by three fans and the convection is therefore forced.

Once the method of heat transfer had been determined, theoretical solutions to problems of this kind were researched. The most relevant solution to the case being investigated was an approximate solution of heat distribution in a hemisphere subjected to forced convection that was proposed by L. M. Chiapetta and D. R. Sobel.[4] The solution was obtained during their research into the thermal integrity of the tip region of a gas sampling probe in which the flat surface of the tip was kept at a constant temperature and the curved section exposed to a hot flow of gas, the solution is presented as a series of Legendre polynomials.

The solution to the hemisphere temperature distribution requires the heat transfer coefficient to be know and this can be calculated using the correlation proposed by Whittaker [1]. This correlation uses the Nusselt number to calculate the heat transfer coefficient. The Nusselt

number is a dimensionless number that represents the enhancement of heat transfer through a fluid layer as a result of convection relative to conduction across the same layer [1]. The Reynolds number of a flow relates to the turbulence in the flow and is one of the factors used to determine the Nusselt number.

Computational Fluid Dynamics in Food Processing[5] describes the work that has been carried out in the food industry using CFD, problems that occur when over simplifying problems and techniques to increase simulation accuracy. The most relevant points to the case being studied were about meshing and problems with simplification. It discusses the benefits of using unstructured hexahedral meshing and how it has led to increases in simulation accuracy in the food industry, it states that this is one of the benefits of using ANSYS Fluent code as it is able to use this meshing technique. It continues to discuss the problems that have been found when simplifying models, and states that simplifying three dimensional scenarios into two dimensions often leads to inaccuracies. Finally turbulence models are discussed and although modern variants of the k-ε model have been found to be more accurate than the standard k-ε model in some cases, it concludes that the standard k-ε model can still be relied upon to produce accurate results.

Fluid Mechanics[6] was referred to for two formulas, the first being the equation to determine the velocity from the pressures given by a pitot static tube and the second being the equation to calculate the Reynolds number of a flow.

When determining how to connect the temperature sensors to the Arduino the TMP36 datasheet [7] was referred to.

3. Methodology and theory

In order to create a reliable CFD model of a Cornish pasty there needs to be a method to validate the results and show the models accuracy. Due to difficulties in validating the complex shapes the investigative work in this project will initially make simplifications which will allow theoretical and experimental analysis to be carried out. These simplified shapes can then be used to validate similar but more complex cases.

3.1. Theoretical Temperature Distribution in a Hemisphere Exposed to a Vertical Flow of Air

The temperature distribution in a hemisphere that is exposed to a vertical flow of air is able to be calculated theoretically and this will be used to validate the modelling in this project. The temperatures in the hemisphere were calculate along 3 different radii at $\theta = 0$, $\theta = \frac{\pi}{3}$ and $\theta = \frac{\pi}{6}$ shown in figure 1 with 10 data points at even intervals on each line.

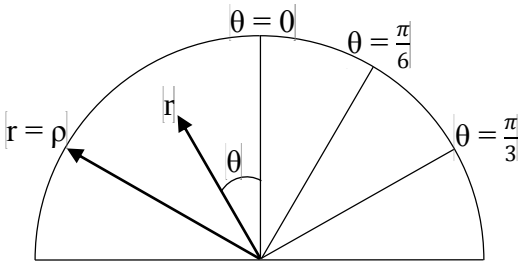

Figure 1 – Diagram of hemisphere.

3.1.1. Heat Transfer Coefficient

In order to calculate the temperature distribution in the hemisphere the heat transfer coefficient was obtained. To find this, the Reynolds number and the Nusselt number for the hemisphere were calculated using Equations 1 and 2. Equation 2is the Whitaker relationship and is used to calculate the Nusselt number for flow over a sphere and is valid for 3.5 < Re < 80,000 and 0.7 < Pr < 380. It is acceptable to use the Whitaker relationship, which is for spheres, in the case being investigated as only the curved section of the hemisphere is transferring heat and will, therefore, have the same Nusselt number as a sphere.

$$Nu_{sph} = 2 + \left(0.4Re^{\frac{1}{2}} + 0.06Re^{\frac{2}{3}}\right) Pr^{0.4} \left(\frac{\mu_\infty}{\mu_s}\right)^{\frac{1}{4}}$$

Equation 1 – Whitaker Relationship; Nu is the Nusselt number, Re is the Reynolds number, Pr is the Prandtl Number, μ_∞ is the dynamic viscosity at the free stream temperature, μ_s is the dynamic viscosity at the surface temperature.

$$Re = \frac{\rho v D}{\mu}$$

Equation 2 – Reynolds Number; Re is the Reynolds number, ρ is the density of air, v is the velocity of the flow, D is the diameter of the hemisphere, μ is the dynamic viscosity.

The values obtained for the Reynolds number and Nusselt number were then used to calculate the heat transfer coefficient for the hemisphere using Equation 3.

$$h = Nu \frac{k}{D}$$

Equation 3 – Heat Transfer Coefficient; Nu is the Nusselt Number, k is the thermal conductivity of air, D is the diameter of the hemisphere.

3.1.2. Temperature Distribution

Once the heat transfer coefficient was calculated the temperature distribution in the hemisphere could then be calculated. This was done using Equations 4, 5 and 6 which were solved using MATLAB script shown in figure 2and where z = cos (θ).

$$T(r,z) = T_c + \sum_{m=0}^{\infty} C_m r^{2m+1} P_{2m+1}(z)$$

Equation 4 – Temperature Distribution in a Hemisphere; T is the temperature, r see figure 1, z see figure 3, T_c is the temperature of the base of the hemisphere, C_m is a constant, $P_n(z)$ is the Legendre polynomial of order n.

$$C_m = \frac{B_m}{\left(\frac{(2m+1)k}{\rho h} + 1\right)\rho^{2m+1}}$$

Equation 5 – Constant C; B_m is a constant, k is the thermal conductivity of the hemisphere, ρ see figure 1, h is the heat transfer coefficient.

$$B_m = \frac{(-1)^m (2m)!\,(T_G - T_c)(4m+3)}{2^{2m+1}(m+1)(m!)^2}$$

Equation 6 – Constant B; T_g is the temperature of the air, T_c is the temperature of the base of the hemisphere.

```
function [Trz] = t(r,z)

Tg = 293.15;
Tc = 333.15;
k = 0.19;
rho = 0.05;
h = 42.4;
mstrt = 0;
mend = 84;
x = 0;

for m = mstrt:mend
    x = x + c(m,Tg,Tc,k,rho,h)*r^(2*m+1)*legendreP((2*m+1),z);
end

function [Cm] = c(m,Tg,Tc,k,rho,h)
    Cm = b(m,Tg,Tc)/(((((2*m + 1)*k)/(rho*h))+1)*rho^(2*m+1));
end

function [Bm] = b(m,Tg,Tc)
    Bm = (((-1)^m)*(factorial(2*m))*(Tg - Tc)*(4*m + 3))/((2^(2*m+1))*(m + 1)*((factorial(m))^2));
end

Trz = Tc + x;
end
```

Figure 2 – MATLAB Script to calculate temperature distribution

3.2. Experimental Method

The experimental work for this project was carried out in a wind tunnel using an expanded polystyrene hemisphere representing a pasties. The model was inserted into the wind tunnel and the airflow was then switched on. A pitot tube and a static pressure source were then used to find the velocities at the inlet and outlet of the working section. The total pressure and static pressure was recorded at five locations at the inlet, shown in blue in figure 3, and twenty-five locations at the outlet, shown in red in figure3. In order to obtain the velocity from the total pressure and the static pressure Equation 7 was used.

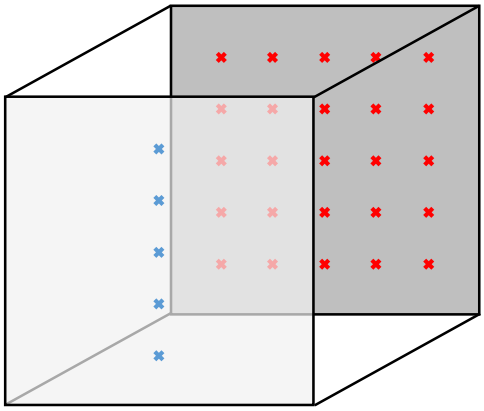

Figure 3 – Locations where total and static pressure were recorded.

$$u = \sqrt{\frac{2(p_t - p_s)}{\rho}}$$

Equation 7 – Airflow Velocity; u is the velocity, p_t is the total pressure, p_s is the static pressure, ρ is the density.

The ceramic heating element was then switched on and heated to 330K by applying 6.2V through it. The temperatures in the model were monitored using command prompt and were recorded once they had stabilized. The heating element was then switched off before the models were rotated and the heating procedure carried out again. The hemisphere was rotated three times by 90° each time to allow data to be recorded at all of the required points.

3.3. Temperature logging

The temperatures inside of the model was recorded using six TMP36 temperature sensors connected to an Arduino UNO. The TMP36 has a scale factor of 10mV/°C and provides a 750mV output at 25°C. The program that the Arduino was loaded with produced an integer between 0 and 1023 which was proportional to the input between 0 and 5V. This information was used to derive Equation 8 which converts the output to Kelvin.

$$T = 298.15 + \left(\frac{\left(\frac{O}{1024} \times 5 \right) - 0.75}{0.01} \right)$$

Equation 8 –Arduino Output to Temperature Conversion; T is the temperature in K, O is the output.

3.4. Computational Method

3.4.1. Modelling the Geometry and Meshing

ANSYS Fluent was used for the simulations and meshing and SolidWorks was used for making the geometry for the simulations. The models were created in SolidWorks and imported into the ANSYS Design Modeller instead of being made exclusively in the design modeller software due to it being unintuitive and difficult to use. In order for the Design Modeller software to differentiate between the physical models and the volume for the airflow they had to be made as separate parts on SolidWorks and then imported as frozen bodies. Once the parts had been imported named selections were made for the inlet, outlet, heated base and the interfaces between the air and the model so that boundary conditions could be applied. There were three different physical models used in the simulations with the first being the 100mm diameter hemisphere shown in figure 4.

The second model, shown in figure 5, was a solid pasty that was 100mm long, 25mm high and had a curved section of radius 60mm. A curved profile was cut along the pasty to more closely resemble the pasties sold by Ginsters.

The third model was a composite pasty comprised of three parts - the first represented the pastry and was a 2.5mm thick shell that had the same outer dimensions as the previous model. The second part, representing the filling, was 90mm long, 20mm high and had a curved section of radius 50mm. The final part was created from the space in between the two previous parts and represented the air inside the pasty. This model can be seen in figure 6.

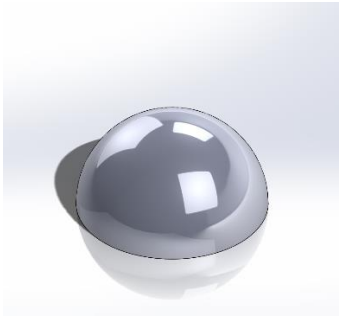

Figure 4 - Hemisphere

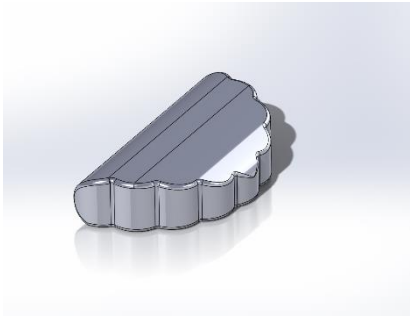

Figure 5– Solid Pasty

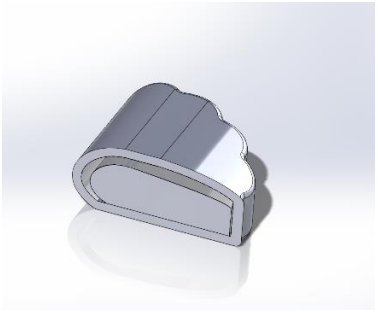

Figure 4 – Composite Pasty

In order to find a suitable mesh for the simulations two mesh convergence studies were run for the hemisphere in a vertical flow of air. The first was run on the mesh for the airflow with mesh size between 25mm and 2.5mm, the mesh for the hemisphere was kept at a constant 1mm so that any change in the result were due to the airflow mesh changing. The quantity of interest for the airflow is the velocity and so this was recorded for each simulation to check for convergence. The results from the first mesh convergence study can be seen in Table 1 and the graph of the average outlet velocity against the number of elements in Figure 7.

Mesh Size (mm)	No. of Elements	No. of Nodes	Av. Outlet Velocity (m/s)
25	5692	1209	12.356
15	20940	4155	12.448
10	67135	12576	12.471
5	536135	95112	14.478
3.5	1556080	270800	12.479
2.5	4270883	736402	12.479

Table 1 – Results of the mesh convergence study of the air flow.

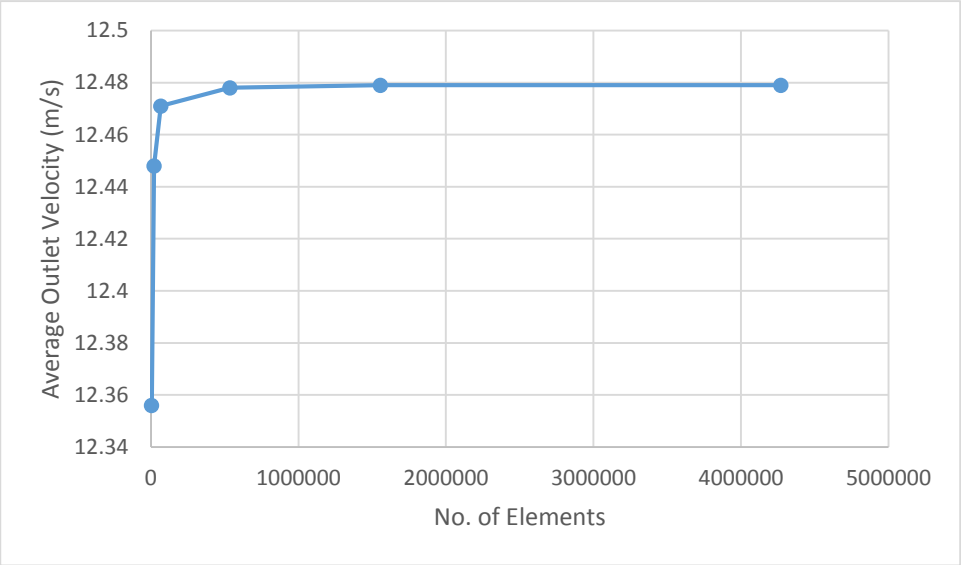

Figure 5 – Graph of the average outlet velocity against the number of elements in the mesh convergence study of the airflow.

From this data a mesh of 5mm was chosen for the air as the optimum size because it is sufficiently small to ensure accuracy without having excessive computational times. This mesh size of 5mm was used for the air in the mesh convergence study of the hemisphere. In this study the mesh was varied in size between 10mm and 0.5mm. The quantity of interest in the hemisphere is the temperature so the average temperature of the hemisphere was recorded for each mesh size. The results for the second mesh convergence study can be seen in Table 2 and a graph of the average temperature of the hemisphere against the number of elements in Figure 8.

Mesh Size (mm)	No. of Elements	No. of Nodes	Av. Temperature (°C)
10	4744	1066	311.597
5	18272	3614	309.303
2.5	146331	26710	309.423
1.5	670942	118361	309.467
1	2261137	392056	309.486
0.75	5352389	920084	30.500

Table 2 – Results of the mesh convergence study of the hemisphere.

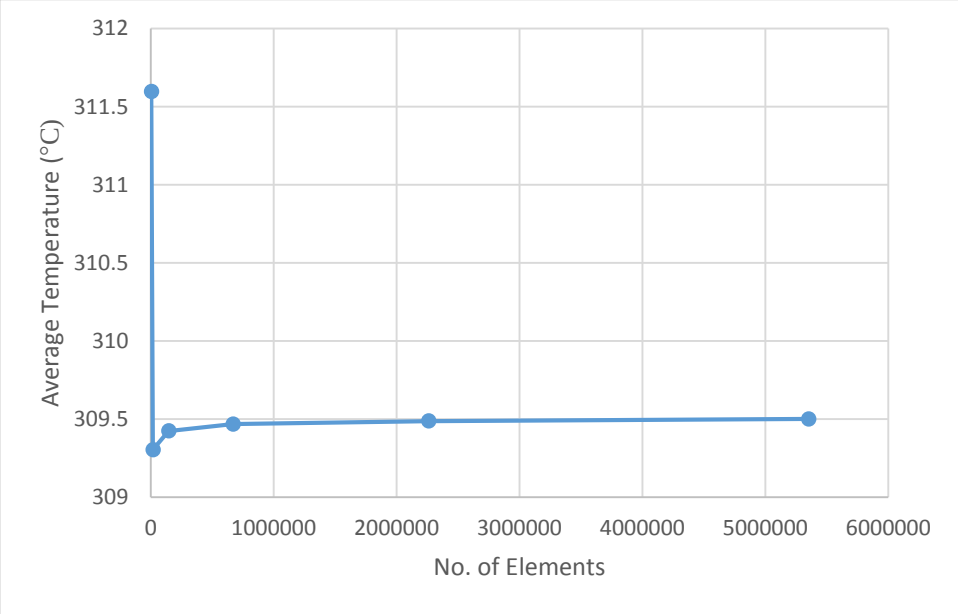

Figure 6 – Graph of the average temperature against the number of elements in the mesh convergence study of the hemisphere.

From these results a mesh of 1mm was chosen for the hemisphere as the result had converged at this point and a smaller mesh would only result in longer simulation times with an insignificant increase in accuracy. The mesh sizes determined from this study were used for all of the simulations carried out, the hemisphere mesh was used for all solid objects and the air mesh for all the air flows. These mesh sizes was suitable to use for the main bodies in all of the simulations, however, finer meshes had to be added on to the curved sections on the solid and composite pasties.

3.4.2. Setup and Boundary Conditions

In order to determine whether a turbulence model was necessary for the simulations the Reynolds numbers for each of the scenarios were calculated using Equation 2 in section 3.1.1. The Reynolds number for the flow over the hemisphere and the pasty was 60,271 due to both

cases having the same characteristic length. Both of these flows are turbulent as their Reynolds number are greater than 4000 and because of this a turbulence model was needed. The k-epsilon model was chosen as it performs well in external flow problems over complex geometries such as the cases being investigated, it also suitable model as it does not have high computational requirements in comparison with other turbulence models. In addition to a turbulence model, the energy equation was used allowing heat transfer to be modelled. Interfaces between the different parts of the models also had to be set up to ensure heat transferred correctly across the boundaries.

In total six different cases were simulated and the boundary conditions used in each case can be seen in table 3.

Simulation No.	Physical Model	Flow Direction Vector	Inlet Temperature (K)	Inlet Velocity (m/s)	Heating Element temperature (K)
1	Hemisphere	(0,-1,0)	296.15	10	333.15
2	Hemisphere	(1,0,0)	296.15	10	333.15
3	Hemisphere	(1,0,0)	296.15	10	333.15
4	Hemisphere	(1,0,0)	245.15	10	344.26
5	Solid pasty	(1,0,0)	245.15	10	344.26
6	Composite pasty	(1,0,0)	245.15	10	344.26

Table 3 – Simulation Boundary Conditions

The first set of simulations were run with boundary conditions reflecting the conditions of the experiment to allow the results to be directly compared. The experiment was run with simplified conditions of those found in the Ginsters factory because the experimental apparatus available was not equipped to reach the same temperatures. Once the simplified simulations had been validated with experimental and theoretical data, the boundary conditions were adjusted to reflect the actual conditions at Ginsters.

Simulation No.	Fluid	Solid Material	Solid Density	Specific Heat	Thermal Conductivity
1	Air	EPS	15 [8]	1130 [9]	0.038 [8]
2	Air	EPS	15	1130	0.038
3	Air	ABS	1080 [10]	1675[10]	0.19[10]
4	Air	ABS	1080	1675	0.19
5	Air	ABS	1080	1675	0.19
6 – Pastry	Air	Bread	161.4[11]	0.0989[12]	2930[11]
6 - Filling	Air	Ground Beef	1024[13]	3520[14]	0.41[13]

Table 4 – Simulation Material Properties

Due to complications with 3D printing detailed in section 4.6 expanded polystyrene was used in the experiments instead of ABS, and so in the simulation of the experiment EPS was also used. It was decided to still use ABS as the material in the other experiments as EPS is more highly thermally insulating than ABS and so is less similar to a pasty. The exact thermal and physical properties of pastry and pasty filling could not be found so the properties of bread and cooked minced beef were used as an approximation.

The final stage before running the simulations was setting the residual monitors to an absolute criteria of 0.00001 in order to check for convergence of the solution. Once the simulations were completed the airflow velocities were recorded at the outlet and the inlet and the temperatures recorded at multiple points throughout the solid model.

4. Experimental design

In order to carry out the proposed experimental work several pieces of apparatus had to be custom designed and manufactured. The process through which this was carried out is detailed below.

4.1. Working Section Design

The working section needed to be fitted onto a wind tunnel and this therefore gave some initial constraints for the design. The mounting points for the working section are shown in Figure 9, the external square is 162.5mm x 162.5mm, the internal square is 124.5mm x 124.5mm and the distance between the two mounting points is 200mm.

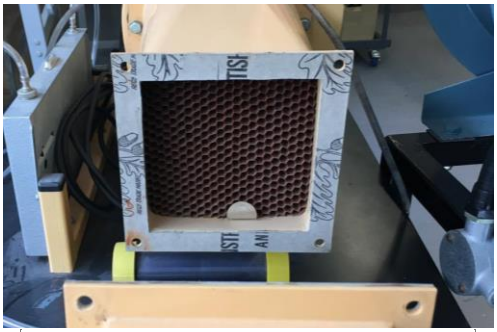

Figure 7 – Mounting point for working section.

The working section is secured to the mounting points with 4 x 7mm bolts at each end.

The sensors and measurement device used in the experiment are another crucial design factor. In the experiment a pitot tube and a static pressure source were used to measure the static and total pressures at the locations shown in Figure 3 in section 3.2. The pitot tube used in the experiment requires a 12.5mm hole to be inserted into and a 6mm hole for a pin to ensure the pitot tube is in the correct orientation. There are six locations that the pitot tube needed to be placed, one at the inlet and five at the outlet, so holes were made at these locations. The static source requires a 5mm diameter threaded hole that is 7.5mm deep with a 1.5mm hole through the bottom of it into the main area of the working section. The static source is only required to be measured once at the inlet and once at the outlet so one hole was required at each of these locations. Temperature sensors and a heating element were also required inside the working section and so wires leading to these needed a place to enter the working section, a 10mm hole was added to allow for this. Based on these constraints and requirements a design was created on SolidWorks that was comprised of four flat pieces that were assembled to create the working section. The design is shown in Figure 10.

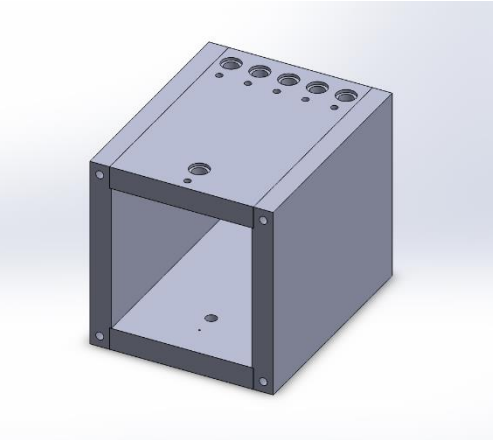

Figure 8 – Working section design

4.2. Working Section Material Selection

In order to decide the most suitable material for the construction of the working sections the objectives and constraints were looked at. These were as follows: the material must be see-through so the experiment can be observed, it must be able to be machined and joined using university workshop equipment, it should be low cost to ensure the project can operate within budget and it should be robust enough so that it will not be damaged when being moved around the workshop and aerodynamics laboratory. Three materials were selected as possibilities for the construction and analysed for their compliance with the objectives and constraints, the three materials were glass, acrylic and polycarbonate. Glass was ruled out as a possible material due to the difficulties when machining it. Acrylic and polycarbonate were both suitable for constructions as they both fulfilled all of the criteria, however, due to the higher cost of polycarbonate acrylic was selected.

4.3. Working Section Design Changes

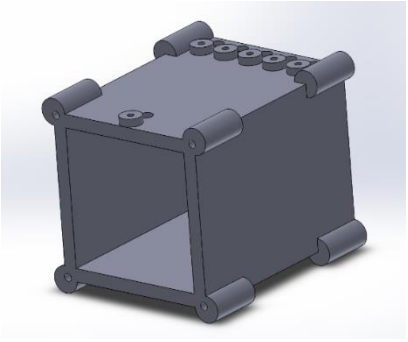

Figure 9 – Design changes to working section.

The initial design was intended to be constructed out of 19mm thick acrylic sheeting, however, due to a lack of availability of this material 12mm thick acrylic was used instead. Due to the reduction in thickness certain aspects of the design had to be altered so that it would still be compatible with the other equipment used in the experiments. The first problem was the threaded holes were used to attach the working section to the mounting point on the wind tunnel over lapping with the edge of the material and so would not be able to be drilled. To correct this circular sections with a step cut out were attached to the corners and these sections were then drilled into and threaded to be attached to the mounting point. Another problem was that the pitot tube was designed to be inserted into a working section with a 19mm wall thickness and when the thickness was reduced the plug around the base of the pitot tube extended into the working section which would have caused a disturbance to the airflow. To counteract this problem a 7mm thick buffer was added around the hole for the pitot tubes alignment pin, this held the base of the pitot tube 19mm from the outer wall of the working section and meant that the plug around the pitot tube was flush with the inner wall. The adapted deign can be seen in Figure 11.

4.4. Working Section Manufacture

The working section was manufactured in the student workshop using a number of different machines and techniques. The sides of the working section were measured and cut to an approximate size using the bandsaw, they were then squared off and cut to the correct size using the milling machine. The locations for all of the necessary holes were marked and a centre punch used to mark the centres, the holes were then drilled using a pillar drill. The side of the box were glued together using Tensol bonding cement, it was applied along the edges and then the sides were clamped together and left overnight to dry. The circular buffers for the pitot tube were made using the lathe and were friction fitted into the

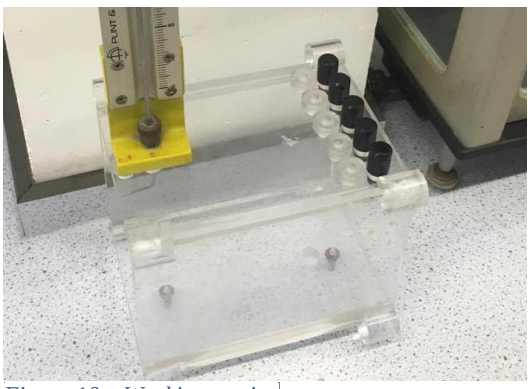

Figure 10 – Working section

holes drilled for them. The circular sections for the bolts to hold the working section to the mounting plates had a step but into them using the milling machine and were then glued to the working section using Tensol. Once the glue had dried the holes for the bolts were drilled and threaded using a tap. The completed working section can be seen in Figure 12.

4.5. Physical Model Design

Although the outer shape of the physical model did not have to be designed as it was a hemisphere, the internal structure to hold the temperature sensors did have to be. The hemisphere was required to contain six temperature sensors – one just above the heating element, one at the top in the centre, two at two points along a line $\frac{\pi}{6}$ radians from the y axis and two at two points along a line $\frac{\pi}{3}$ radians from the y axis. To reduce the effect of the sensors on the heat transfer the four sensors along the angled lines were distributed evenly around the hemisphere, because of this the hemisphere would have to rotated three times by 90° each time in the experiment in order to collect data at all of the relevant points. A cavity also had to be made in the base of the hemisphere for the heating element to be inserted into. The design of the hemisphere with the internal geometry showing can be seen in Figure 13.

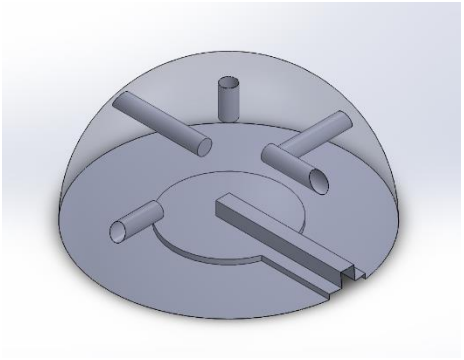

Figure 13– SolidWorks model of hemisphere showing internal geometry

4.6. Physical Model Manufacturing

The model was originally intended to be 3D printed, however, there were a number of problems that occurred with the 3D printing. The first attempt at printing the model was successful, however, it was not printed using the correct settings. The print had an internal lattice structure that can be seen in Figure 14. This was not acceptable as it would change the heat transfer characteristics of the model. A second attempt was made at printing the hemisphere with the correct settings so that it would print a second hemisphere, however, this print was not successful as model warped excessively whilst it was being printed. The reason for the warping was the long time that the printer took to

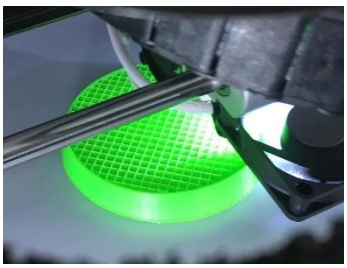

Figure 14 – Hemisphere model

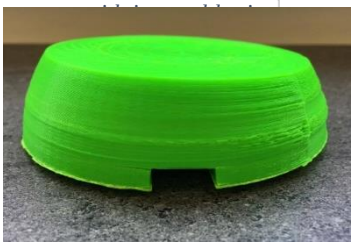

Figure 15 – Warped attempt at printing hemisphere

print each layer which meant sections of the layer cooled and contracted whilst others were still being printed. For this reason the 3D printer was unsuitable for manufacturing the model as it would still have had the problem causing the warping if a print were reattempted. The warping of the model can be seen in Figure 15.

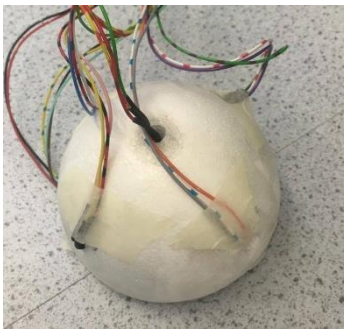

Figure 16– EPS Hemisphere model

The model used in the experiment was made out of an expanded polystyrene sphere. The sphere was first cut in half using a hacksaw and sanded until the base was flat. The locations for the sensor holes were then marked and drilled using a pillar drill. The complete model can be seen in Figure 16.

5. Theoretical, Experimental and Computational Results

5.1. Comparison between theoretical and computational distributions of heat in a hemisphere subjected to a vertical flow

Figure 17 compares the theoretical and computational results for a hemisphere, heated at the base to 333.15K and subjected to a flow of air at 296.15K with a velocity of 10m/s. The graphs shows the decrease in temperature along 3 different radii at $\theta = 0$, $\theta = \frac{\pi}{3}$ and $\theta = \frac{\pi}{6}$, as the distance from the centre of the hemisphere increases.

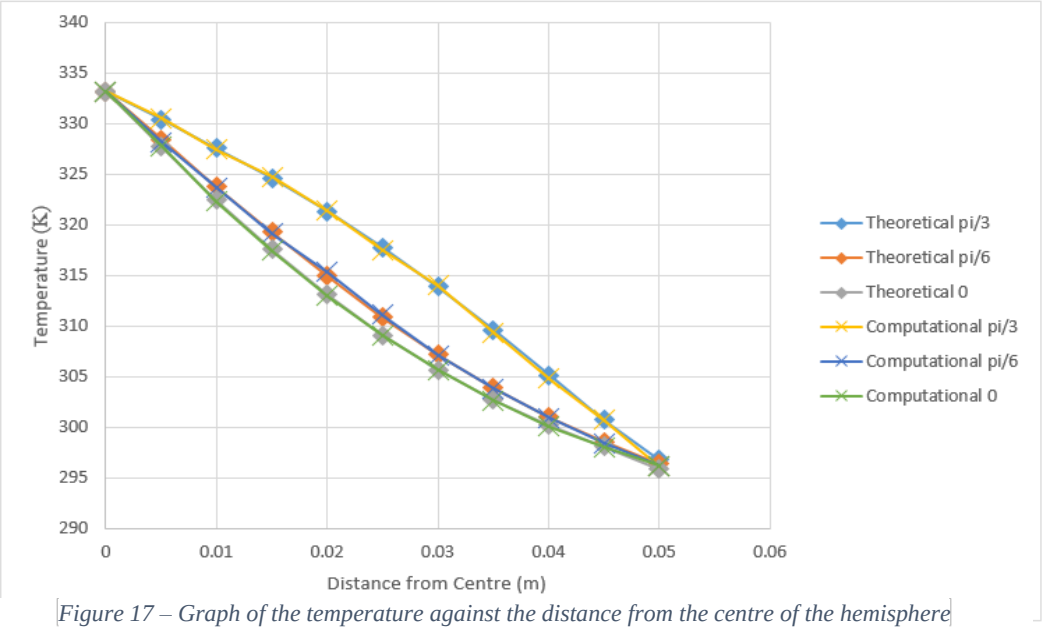

Figure 17 – Graph of the temperature against the distance from the centre of the hemisphere

A strong correlation can be seen between the theoretical and computational results which provides evidence of the accuracy of the CFD simulations when calculating airflows and heat transfer over bluff bodies which is the essential problem being investigated.

5.2. Comparison Between Experimental Data and CFD of a Hemisphere Subjected to a Horizontal Flow.

Figure 18 shows the distribution of temperatures recorded in the experiment, compared with a CFD simulation of the case. Due to limitations with the experimental apparatus it was only possible to collect a small number of data points along three the radii from the centre of the hemisphere. The temperatures recorded along the $\frac{\pi}{6}$ radius in the experiment has a distribution approximately similar to the CFD but with lower temperatures being recorded. There are a number of possible reasons for this discrepancy, firstly the temperature supplied by the heating element in the experiment was 3K lower than in the simulation which will cause a systematic error in the results if compared directly to the simulation. Secondly the heating element used to heat the hemisphere had a diameter of 45mm and therefore only heated the central section reducing the overall heat transferred. This is in contrast with the simulation where the heat was evenly applied to the base of the hemisphere.

Another possible cause is that the internal geometry containing the temperature sensors may have decreased the thermal conductivity of the hemisphere due to trapped air in the sensor slots insulating against the heat. An additional possibility regarding the sensing equipment is that an error occurred due to the soft material the hemisphere was constructed from. If a force was

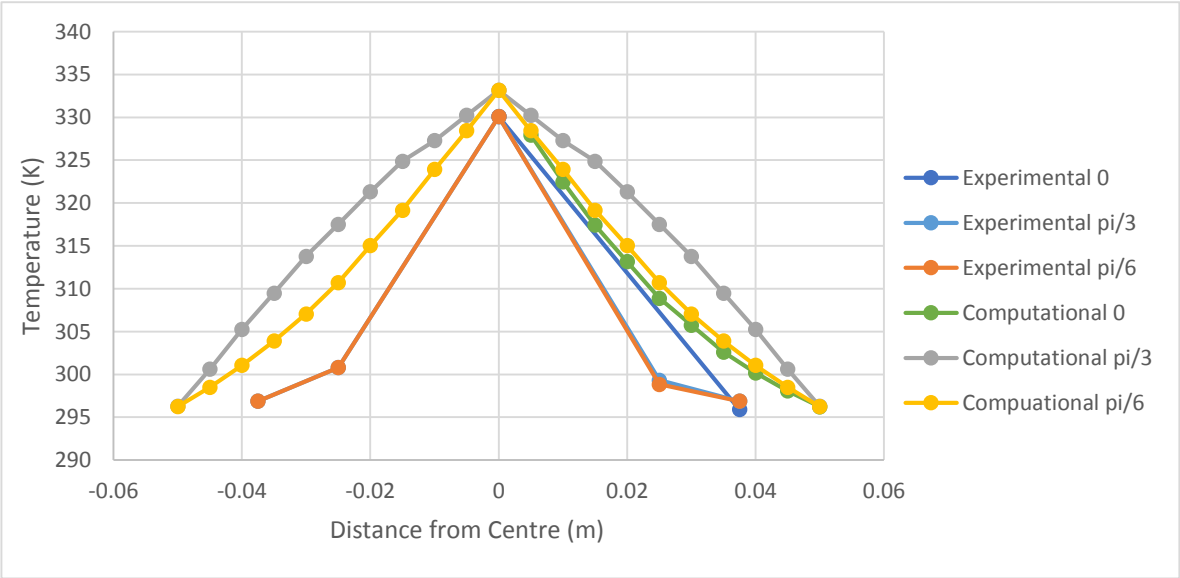

Figure 18 – Graph of Temperature Against the Distance From Centre

applied to the sensors it is possible that a sensor could have compressed the walls of the hemisphere and therefore changed the location the temperature was being measured, if this did occur it would cause a systematic error for dislodged probe.

The differential pressure at the working section inlet was 0.71mbar which gave a velocity of 10.9 m/s, the inlet velocity in the simulation was a slightly lower 10m/s and so would have had less of a cooling effect, however this effect will have been negligible. The outlet velocity of the working section was also attempted to be recorded in order to compare to outlet velocities in the CFD simulation, however, the pressures constantly fluctuated and therefore made it impossible to record an accurate reading.

5.3. Heat Distribution in All Models

The progression of the iterative modelling process can be seen in Figure 19, the simple hemisphere is shown in i, the solid pasty model shown in ii and the composite pasty in iii. The temperature distributions patterns observed in i and ii are consistent with those observed in the experimental and theoretical results, the patterns show even cooling over the pasty and the cooling effect of the airflow penetrating into the centre. iii, however, does not appear to follow this pattern, with heat propagating much further up the pasty.

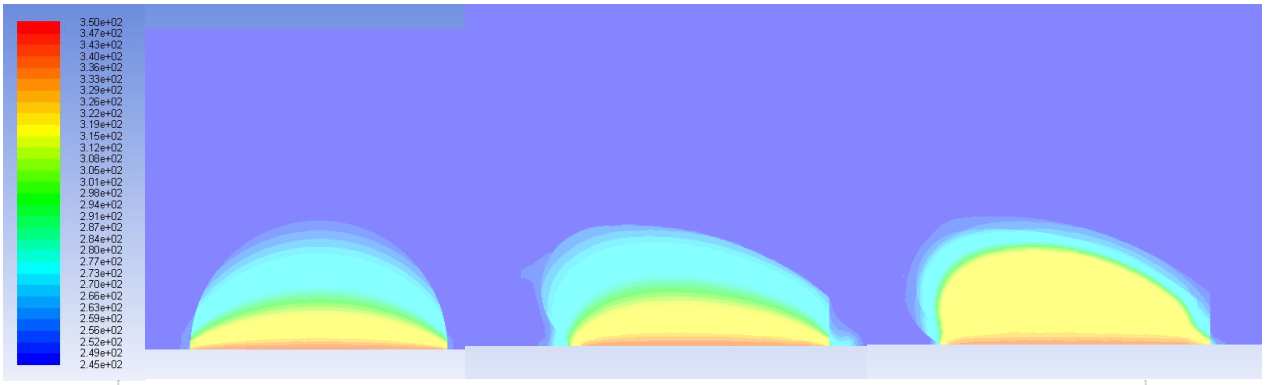

Figure 19 – i) Solid ABS hemisphere ii) Solid ABS pasty iii) Composite pasty comprised of meat and bread

Figure 21 shows the temperatures vertically through the centre of the pasty. Both the solid pasty and the solid hemisphere have relatively linear changes in temperature as the distance increases, however, this is in contrast to the composite pasty. The composite pasty maintains its temperature more effectively as distance increase, until at approximately 0.0225m from the base the temperature starts to decrease at a rapid rate. When the temperature distribution in the composite pasty is aligned with its internal geometry, as shown in Figure 20 can be observed that this is caused by the air pocket surrounding the filling and insulating against the cool

airflow as the temperature rapidly changes from hot to cold over this section.

The insulating property of the air pocket in-between the pastry and filling suggests that the current forced convective technique Ginsters uses for cooling pasties is inefficient. More detailed computational and experimental analysis will need to be carried to determine the accuracy of these findings and assess the implications in terms of energy wastage and financial losses to Ginsters.

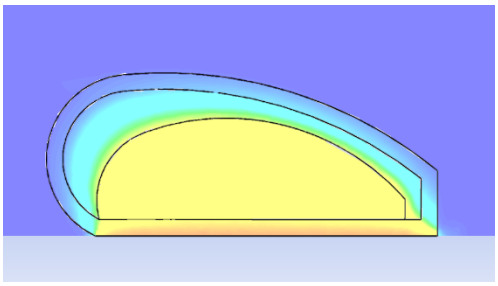

Figure 20 – Distribution of temperature in pasty compared with physical geometry

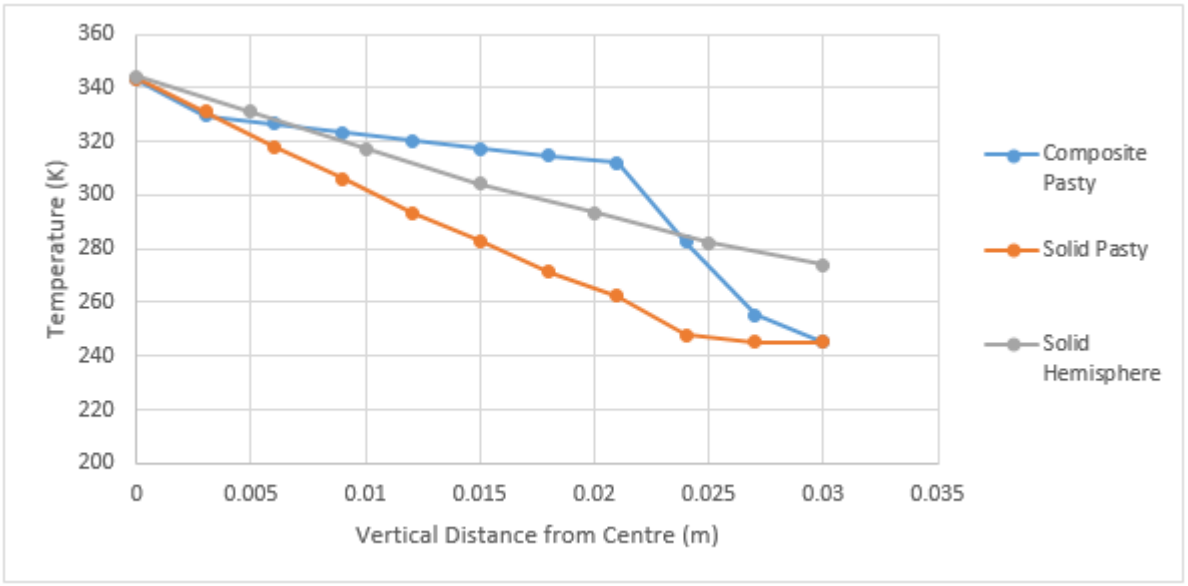

Figure 21 — Graph of the Temperature Against Vertical Distance

6. Discussion and conclusions

The simulation work carried out in this project correlated well with theoretical results and certain aspects of the experimental results, his was positive as it validated the CFD work. The experimental work could have been improved upon if time was spent looking for alternative 3D printing options that were capable of printing the desired geometry rather than using a rough model to reduce the chance of errors. In addition it is useful when planning an experiment to think of problems that could lead to errors before the experiment so that they can be detected early and compensated for.

The final comparison between the three pasty models showed that the simplified models did not function in the same manner as the more advanced one. This shows that for future work carried out, solid models are not suitable as they do not have similar characteristics to pasties even with identical external geometry.

The composite pasty provided useful insight into the effectiveness of the cooling mechanism currently used. Further work need to be carried out to validate the CFD results and ensure that the simulation was accurate and the inside of the pasty was not well cooled. To further refine the CFD model, experimental work should be undertaken to find the specific thermal properties of a Ginsters pasty, in addition a pasty could be scanned to create the geometry for the simulations so the exact shape could be used rather than close approximation.

7. Project management, consideration of sustainability and health and safety

Several methods were used throughout the project to manage its progress and ensure that it would be completed on schedule. A Gantt chart was used to plan out the main phases of the project and was used to provide a clear structure that, if followed, would ensure the project was completed before the deadline. The original Gantt chart that has been updated with revised dates for some activities, is shown in figure 23.

A log book was also used to provide a convenient medium for ideas and notes to be collected and was continually referred to throughout the project. Regular meetings were held with the project supervisor to discuss the direction of the project and ensure sufficient progress was being made, after the meetings the ideas discussed were written up into the log book so that suggestions and advice could be referred to as work progressed.

In addition to a Gantt chart and log book another tool that was used to aid with the project management was a risk assessment form. The risk assessment was used for two purposes – firstly to assess the potential physical dangers that could arise in the project, specifically from the manufacturing and experimental work, and secondly, to prepare for problems which could lead to delays and compromise the ability for the project to be completed on time.

Once the physical hazards, ID. 1-4 in figure 22, had been assessed actions were determined to mitigate the chances of the risks. Firstly safety glasses and a lab coat were worn at all times in the workshop and aerodynamics lab, this was to protect the eyes from airborne debris and to keep avoid losing clothing being pulled into machinery. Before the heating element was connected to a power supply it was attached to a temperature sensor, this allowed the operator in the experiments to check it was not dangerously hot before handling it. In addition to this, the power was restricted to the heating element in order to maintain temperatures below 60°C and reduce the chance of burns.

The simplest was to combat the problems that would lead to delays was to start on these sections, specifically the manufacturing, at an early date. This was attempted, however, the time necessary to manufacture components was underestimated and this led to them not being

completed in the workshop time allocated. As a result of this the manufacturing had to be delayed until 11th April which caused the experimental work to also be delayed. In an attempt to combat this delay, the work that could be carried out regardless of the experimental results was conducted and written up. Spreadsheets were also prepared that would allow quick, efficient analysis of the results, once the experiments were conducted on the 25th April. This

Risk Assement						
Name of person carrying out risk assesment			Oliver Nield			
Description:			An investigation into the heat distribution of a pasty will be carried out, this risk assesment will cover manufacturing, experimental work and report			
ID.	Hazard	Who and How Many can be	How can they be harmed?	Consequence	Likelihood	Risk Score
1	Injuries sustained from misuse of workshop machinery.	The operator of the machine.	Crushing or tearing injuries, eye damage.	4	2	8
2	Fire caused by heating element in experiment.	The operator and occupants of the builiding the experiment is in.	Burns, smoke inhilation, death.	5	1	5
3	Loose cloothing sucked into wind tunnel.	Wind tunnel operator.	Equipment damage.	1	3	3
4	High temperatures of heating element.	Experiment operator.	Burns.	3	3	9
5	Loss of work.	Student carrying out project.	Loss of data reducing the likelihood of project being completed on time.	4	2	8
6	Workshop fully booked in term time.	Student carrying out project.	Delays to construction of experimental equipment.	3	2	6
7	3D printer fully booked in term time.	Student carrying out project.	Delays to construction of experimental equipment.	3	3	9
8	Difficulties with ANSYS due to software unfamiliarity.	Student carrying out project.	Unable to conduct computational work.	3	2	6

Figure 22 – Risk assessment form

permitted the remainder of the report to be written up swiftly and the project completed on time

Task Name	Duration	Start	Finish
Start of Term	75 days	Fri 15/01/16	Thu 28/04/16
Project Supervisor Meetings	75 days?	Fri 15/01/16	Thu 28/04/16
Research	**10 days**	**Mon 18/01/16**	**Fri 29/01/16**
Background Reading	10 days	Mon 18/01/16	Fri 29/01/16
Theoretical Calculations	**8 days**	**Mon 01/02/16**	**Wed 10/02/16**
Initial Calulations	2 days	Mon 01/02/16	Tue 02/02/16
Writing MATLAB Script	3 days	Wed 03/02/16	Fri 05/02/16
Analysing Results	2 days	Mon 08/02/16	Tue 09/02/16
Design	**9 days**	**Wed 20/01/16**	**Mon 01/02/16**
Production of 3D models	6 days	Wed 20/01/16	Wed 27/01/16
Production of Working Drawings for Manufacture	3 days	Thu 28/01/16	Mon 01/02/16
Manufacturing	**59 days**	**Tue 02/02/16**	**Fri 22/04/16**
Working Section	34 days	Tue 02/02/16	Wed 20/04/16
Physical Model	5 days	Mon 21/03/16	Wed 13/04/16
Electronics	1 day	Thu 21/04/16	Thu 21/04/16
Heat Transfer Experiment	**2 days**	**Fri 22/04/16**	**Mon 25/04/16**
Setting up Apparatus	1 day	Fri 22/04/16	Fri 22/04/16
Conducting Experiment	1 day	Mon 25/04/16	Mon 25/04/16
Computational Work	**20 days**	**Mon 28/03/16**	**Fri 22/04/16**
Creating 3D Models	5 days	Mon 28/03/16	Fri 01/04/16
Running Simulations	10 days	Mon 04/04/16	Fri 15/04/16
Analysing Results	5 days	Mon 18/04/16	Fri 22/04/16
Final Report	**14 days**	**Mon 11/04/16**	**Thu 28/04/16**
Writing of Final Report	12 days	Mon 11/04/16	Tue 26/04/16
Formating and Checking References	2 days	Wed 27/04/16	Thu 28/04/16

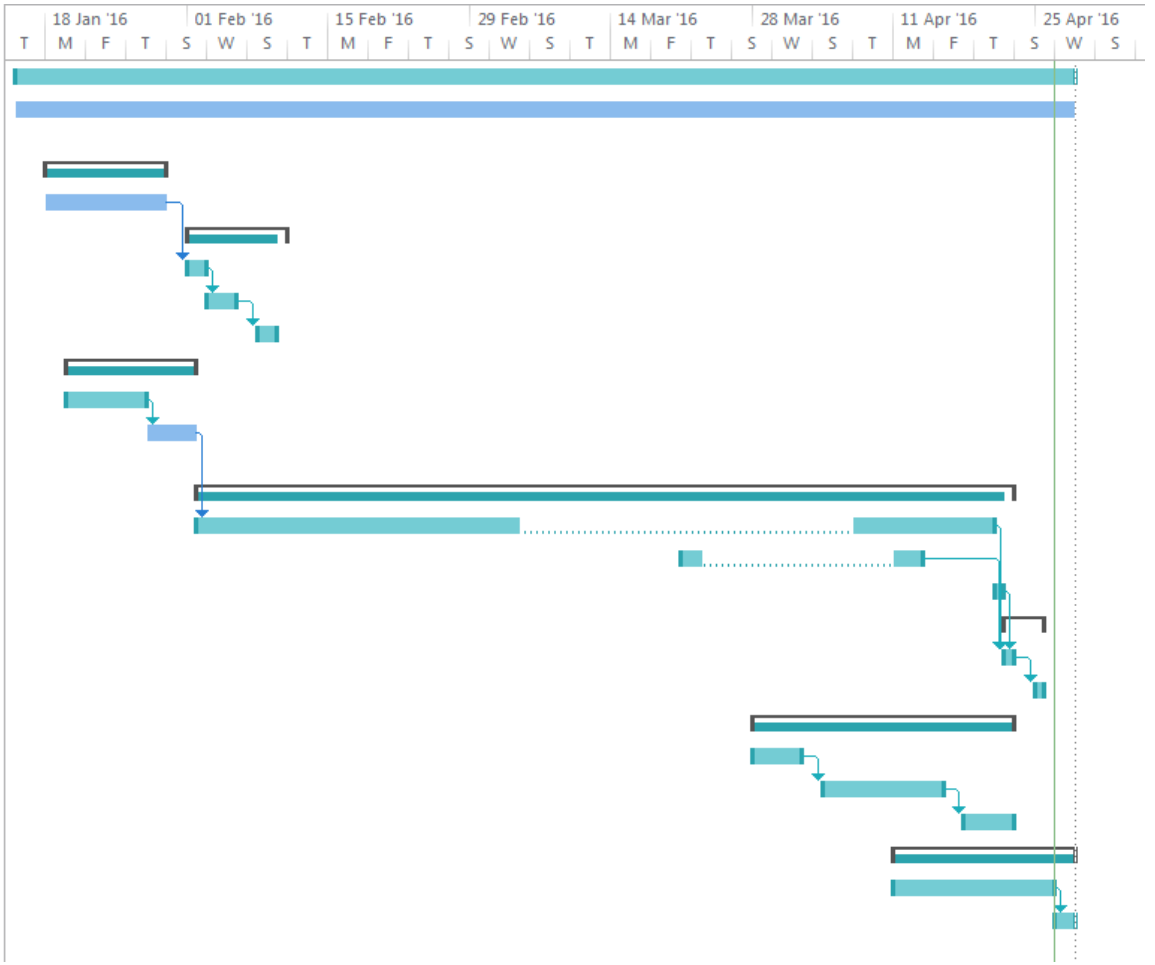

Figure 23 – Gantt chart

References

[1] Yunus A Cengel (2002). *Heat Transfer A Practical Approach*. 2nd ed. New York: Mc Graw Hill. 336,385,.

[2] Kreith, F (2009). *Principles of Heat Transfer*. Boston: Cengage Learning. p546.

[3] R. K . Singal (2013). *Engineering Thermodynamics*. Karnataka: IK International Publishing House. 14.19.

[4] L. M. Chiapetta, D.R. Sobel (1984). *The Temperature Distribution Within a Hemisphere Exposed to a Hot Gas Stream*. Philadelphia: SIAM Review. 575-577.

[5] De-Wen Sun (2007). *Computational Techniques in Food Processing*. Boca Raton: CRC Press. 17-23.

[6] R. K. Bansel (2008). *Fluid Mechanics*. Delhi: Laxmi Publications. 207.

[7] Analog. (2014) *Technical Data Sheets.* [Online] Available from: http://www.analog.com/media/en/technical-documentation/data-sheets/TMP35_36_37.pdf

[8] PACS Packaging. (2015) *Data Sheet for Expanded Polystyrene.* [Online] Available from: http://www.pacspackaging.co.uk/DATASHEETS/Polystyrene.pdf

[9] Isoclad. (2015) *EPS Technical Information.* [Online] Available from: http://www.isoclad.co.uk/pdf/EPS_Datasheet.pdf

[10] Matbase. (2003) *ABS General Purpose.* [Online] Available from: http://www.matbase.com/material-categories/natural-and-synthetic-polymers/commodity-polymers/material-properties-of-acrylonitrile-butadiene-styrene-general-purpose-gp-abs.html#properties

[11] Science Publishing Group. (2014) *Advances in Bioscience and Bioengineering.* [Online] Available from: http://article.sciencepublishinggroup.com/pdf/10.11648.j.abb.20140202.12.pdf

[12] NZIFST. (2012) *Material and Energy Balances.* [Online] Available from: http://www.nzifst.org.nz/unitoperations/matlenerg3.htm

[13] Research Gate. (2015) *Physical and Thermal Properties of Ground Beef During Cooking.* [Online] Available from: https://www.researchgate.net/publication/222784800_Physical_and_Thermal_Properties_of_Ground_Beef_During_Cooking

[14] Engineering Toolbox. (2015) *Food and Foodstuff – Specific Heats.* [Online] http://www.engineeringtoolbox.com/specific-heat-capacity-food-d_295.html